# *Chapter 4.* An Elliptical-Shaped Rectangular Slot Antenna at 2.48 GHz for Hyperthermia Applications

This chapter is based on the design of an elliptical-shaped ground-loaded rectangular slot antenna for hyperthermia applications at 2.48 GHz.

## 4.1. Introduction

Despite the increased number of cancer cases all over the world, there are only a few research articles reported in the past on microstrip patches at higher ISM bands. The novelty of this proposed structure is operating in a higher ISM band of 2.48 GHz with a comparable value of SAR with two different phantom tissues. In this chapter, an elliptical-shaped microstrip patch antenna was developed and designed to operate at the ISM band frequency of 2.48 GHz to study the SAR performance which will extend further for Hyperthermia applications.

## 4.2. Antenna Design

In this Antenna, we have used a dielectric Rogers RT/duroid 5880 copper laminated substrate of a height of 1.58 mm, a dielectric constant of 2.2, and a loss tangent (tan δ) of 0.0009. Initially, the antenna was designed using the relation of microstrip patch and their equivalent transmission line as shown in Figure 4.1(a) [119, 120]. The dimension of the elliptical patch radiator is given by equation (4.1) [121]. The elliptical patch of major radius R1=45 mm, a concentric annular ring of inner major radius R2= 54 mm, and outer major radius R3= 60 mm, on the dielectric substrate, which reduces the major radius of the patch as shown in Figure 4.1(b). On the bottom side, there are two rectangular orthogonal slots of different lengths having a

width (w) as shown in Figure 4.1(c) that intersects an impedance-matching square slot of side (a) positioned concentrically behind the elliptical patch. The top and bottom sides of the final proposed antenna configuration are illustrated in Figure 4.1(d) and Figure 4.1(e) respectively and the reflection coefficient results associated with each evaluation step are given in Figure 4.2. Slots in the ground plane act like a load that can be used to bring the input impedance point closer to the characteristic impedance when added to the antenna, and rectangular orthogonal cross slots on the ground surface of the antenna allow us to adjust the resonant frequency while maintaining the same occupied area. The geometrical parameters of the proposed structure are shown in Table 4.1.

$$a_{eff} = a[1 + \left(\frac{2h}{a\pi\varepsilon r}\right)\left\{\ln\left(\frac{a}{2h}\right) + (1.41\varepsilon r + 177) + \left(\frac{h}{a}\right)(0.268\varepsilon r + 1.65)\right\}]^{1/2} \quad (4.1)$$

Where, a=semi major axis, h= height of substrate, $\varepsilon_r$=relative permittivity

For ground slot length and width calculation, if $L_s$ is the length of the slot and $W_s$ is the width of the slot, then

The radiation resistance of the slot is given as [108, 109],

$$R_r = \frac{\eta cos^2\alpha}{2\pi}\int_0^{\pi}\left[\frac{\cos\frac{k^2 cos\theta}{2} - \cos\frac{kL_s}{2}}{sin\theta}\right]d\theta \quad (4.2)$$

The total input impedance of the slot is given as [109],

$$Z_{slot} = \frac{\eta^2}{4Z_{cy}} \quad (4.3)$$

Where $Z_{cy}$ is given as [108],

$$Z_{cy} = R_r(kL_s)\text{-j}\left\{120(ln\left(\frac{L_s}{W_s}\right) - 1)cot\frac{kL_s}{2} - X_r(kL_s)\right\} \quad (4.4)$$

Where $R_r$ is the real part and equivalent to the radiation resistance of the slot and $X_r$ is the input reactance of the slot and given as [108],

$$X_r = 30cos^2\alpha\{2S_i(kL_s) + cos(kL_s)[2S_i(kL_s) - S_i(2kL_s) - sin(kL_s)]\left[2C_i(kL_s) - C_i(2kL_s) - C_i\left(\frac{2kW^2}{L_s}\right)\right]\} \quad (4.5)$$

Where$S_i(x)$ and $C_i(x)$ are the sine and cosine integrals defined as,

$$S_i(x) = \int_0^x \frac{\sin(x)}{x} dx \quad (4.6)$$

$$C_i(x) = -\int_0^\infty \frac{\sin(x)}{x} dx \quad (4.7)$$

**Table 4.1** Geometrical parameters of the proposed antenna

| Parameter | Value (mm) | Parameter | Value (mm) |
|---|---|---|---|
| L | 128 | R1 | 45 |
| W | 128 | R2 | 54 |
| $L_1$ | 116 | R3 | 60 |
| $L_2$ | 88 | $R_{in}$ | 0.47 |
| a | 20 | W | 5 |

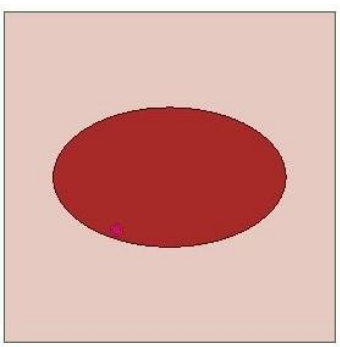

(a)

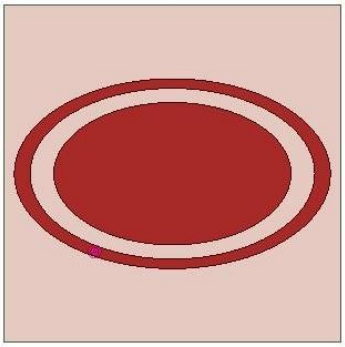

(b)

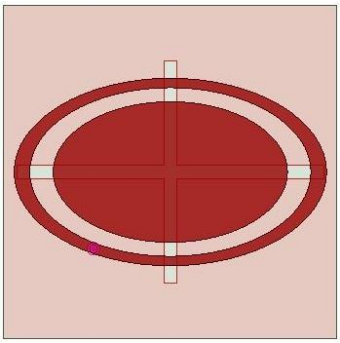

(c)

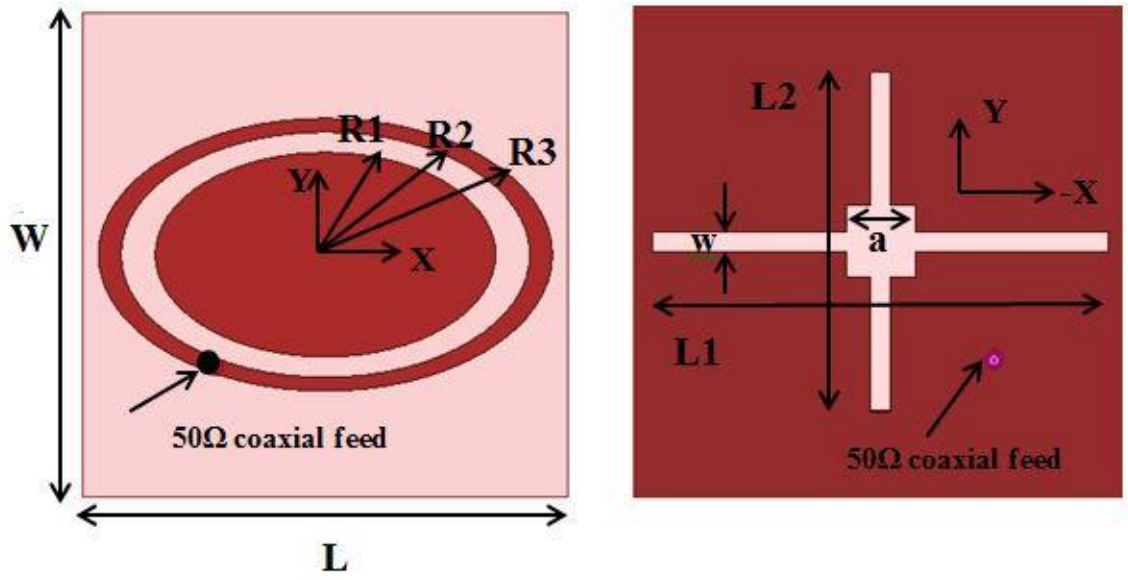


(d) (e)

**Figure 4.1** Evaluation steps of the proposed antenna (a) Antenna-1 (b) Antenna-2 (c) Antenna-3 (d) Proposed antenna top view (e) Proposed antenna bottom view

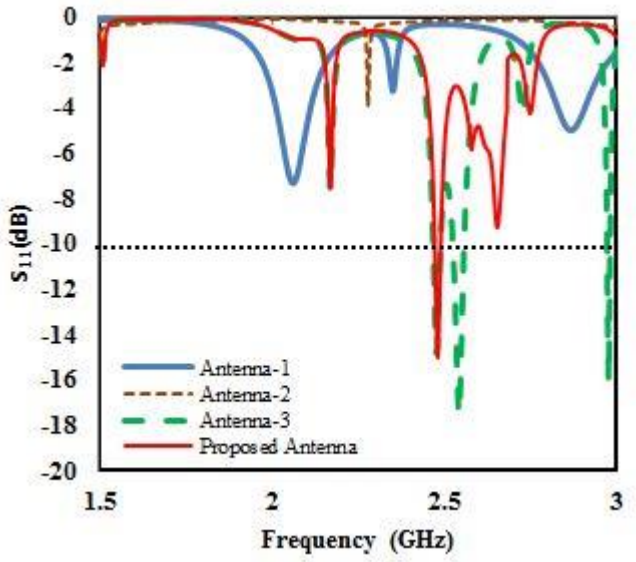


**Figure 4.2** Step-wise simulated $S_{11}$ results of the proposed antenna

## 4.3.Phantom Model

As per IEEE standard, a layered phantom tissue model with water bolus was taken into consideration for DI water and TEL phantoms. We have to make a single-layer

phantom as per measurement availability in the laboratory. Effective permittivity for single layer phantom tissue model is given in equation (4.8).

$$\epsilon_{eff} = (\epsilon_{r1} + \epsilon_{r2})/2 \quad (4.8)$$

Where $\epsilon_{r1}$ and $\epsilon_{r2}$ are the relative permittivity of different layers, using the above equation calculate the effective permittivity of phantom tissue. Parameters of heterogeneous body tissues are described in [56, 113, 119, 122] and the underline geometries with detailed descriptions of the phantom body tissue are available for in-silico analysis [110]. To reduce computational resources and for clarity, a single-layered tissue model was used. The model overloads the antenna fields and provides the main SAR pattern due to the combined strength. Dielectric parameters of DI- water and TEL phantom are, permittivity ($\epsilon_r$) is 77 and 60, conductivity ($\sigma$ S/m) is 1.30246 and 1.83437, and mass density ($\rho$ kg/m$^3$) is 1000 and 1100 respectively to the ISM band [110, 111]. The size of cubical phantoms is 190x130x50 mm$^3$ taking into consideration for simulation as well as during measurement.

## 4.4.Results and Discussion

### 4.4.1. Reflection Coefficient

Figure 4.3(a) shows the value of the simulated reflection coefficient is -15.1 dB and the measured reflection coefficient is -14.9 dB in the case without Phantom. Figure 4.3(b) shows the value of simulated and measured reflection coefficient at different distances of 3cm, 6cm, and 9cm with DI water Phantom. At 3cm simulated and measure $S_{11}$ is -15.67 dB and -20.93 dB respectively, at 6cm simulated and measure $S_{11}$ is -12.74 dB and -11.73 dB respectively, and at 9cm simulated and measure $S_{11}$ is -12.80 dB and -10.03 dB respectively. Similarly, Figure 4.3(c) shows simulated and measured results of $S_{11}$ with the TEL phantom. At 3cm simulated $S_{11}$ is -15.83 dB and measured $S_{11}$ is -11.68 dB, at 6cm simulated $S_{11}$ is -12.24 dB, and measured $S_{11}$ is -10.98 dB, and at 9cm

simulated $S_{11}$ is -15.02 dB and measured $S_{11}$ is -11.09 dB. Figure 4.3(d) shows the measurement setup of $S_{11}$. The antenna is mounted on a stand and connected with the spectrum analyzer (R&S FSH8 100KHz-8GHz) using a probe directly to get the reflection coefficient plot. Now, for the DI water phantom and TEL phantom, fix these phantoms above the antenna and vary with a step size of 3 cm, and get the reflection coefficient results for both the phantom at 3cm, 6cm, and 9cm distance as shown in Figure 4.3(b) and 4.3(c). The differences between the simulated and measured results can be attributed to the manufacturing tolerances, quality of the SMA connector, and scattering environment.

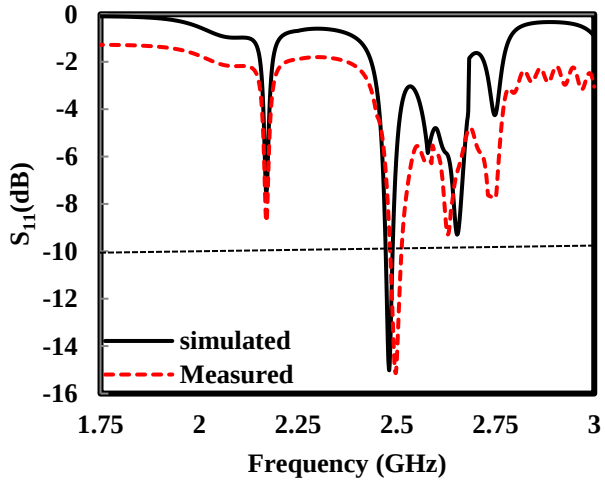


(a) Simulated and measured $S_{11}$ without phantom

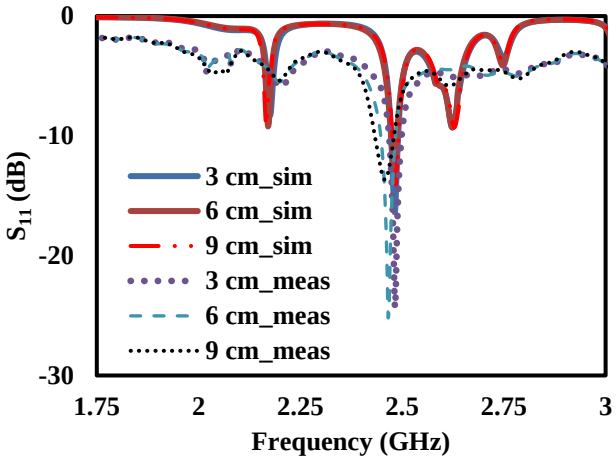


(b) Simulated and measured $S_{11}$ with DI-phantom

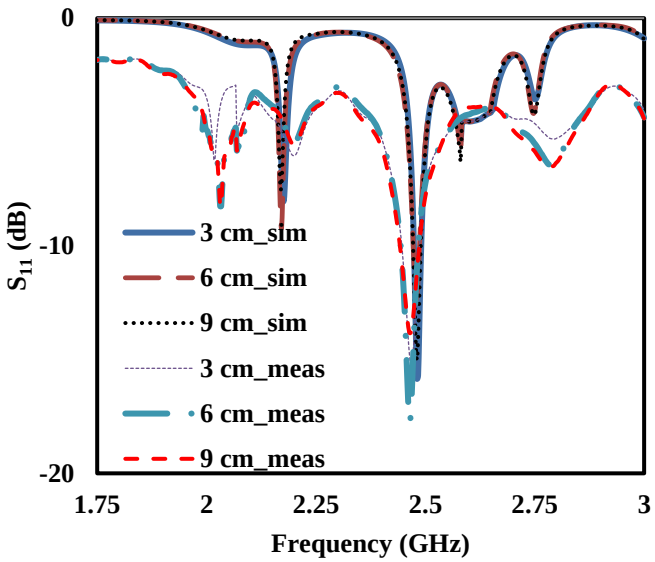


(c) Simulated and measured $S_{11}$ with TEL-phantom

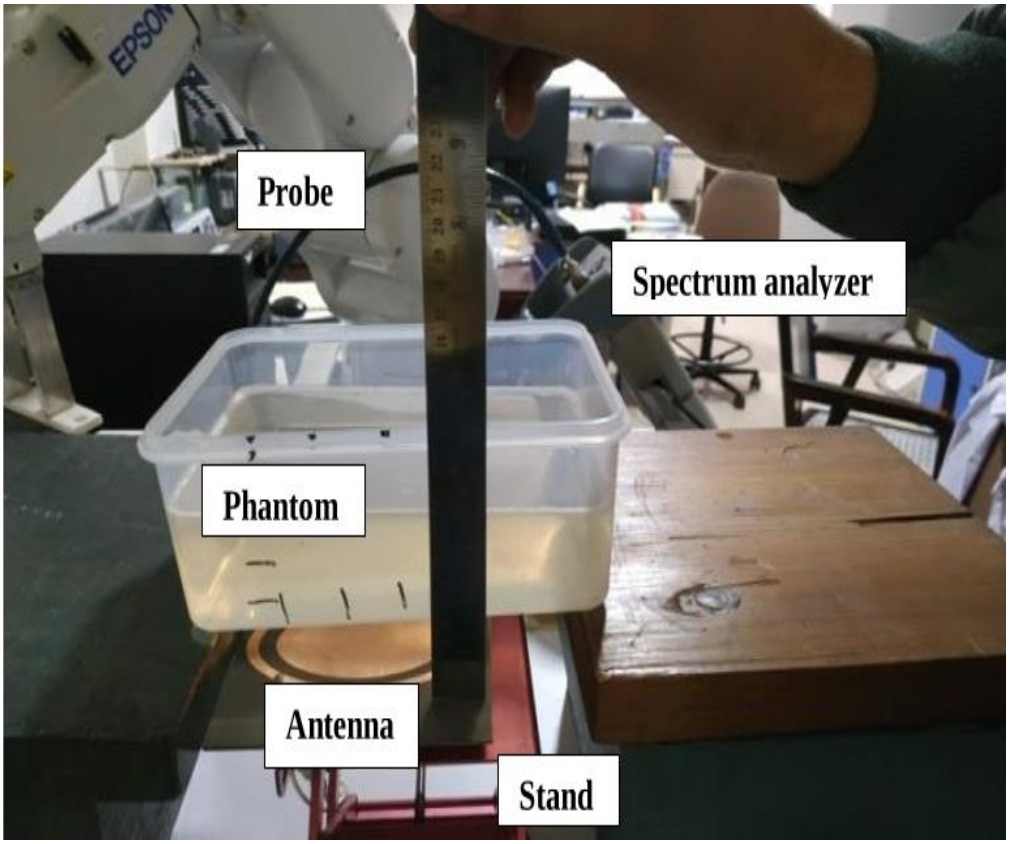


(d) Measurement set up for $S_{11}$

**Figure 4.3** Reflection coefficient results

### 4.4.2. Specific Absorption Rate (SAR)

SAR is determined by measuring Electric Field strength (E) inside the different tissue Phantom materials. In the simulation, we have taken three different cases for SAR calculation. Measurement of E-field strength at different distances is shown in Figure 4.5 and measured values of E-field strength are summarized in Table 4.2. Figure 4.4 shows the variation of the SAR graph w.r.t distances. For measurement of the E-field strength inside the phantoms at different positions, firstly, the power level of the signal generator (R&S SMR SMB100A 10MHz-40GHz) and operating frequency were set to 0 dBm and 2.48 GHz respectively, then antenna and signal generator was connected using a probe. Then, after setting the same frequency in the spectrum analyzer (R&S FSH8 100KHz-8GHz), both the ports of the spectrum analyzer were connected to the Electric Probe [106, 112] and computer. Now, an Electric Probe [106] was inserted into the Phantom tissue of DI water as well as TEL to different positions along the variation of the x-axis penetration depths for E-field strength readings. After getting the E-field strength value, SAR will be given by equation (4.9) in terms of E-field strength, conductivity, and density of the tissue.

$$SAR = \frac{\sigma E^2}{2\rho} \tag{4.9}$$

From Table 4.2, it can be concluded that SAR is the non-linear function of distance. In the case of DI water phantoms, the SAR value is 0.13692 W/kg when E-field strength is measured along the x-axis inside the phantom at a 6.5 cm depth of penetration. In the case of the TEL phantom SAR value is good at 5.13808 W/kg when the E-field strength is measured along the x-axis inside the phantom at 6.5 cm depth, which is suitable for hyperthermia treatment as per IEEE standard.

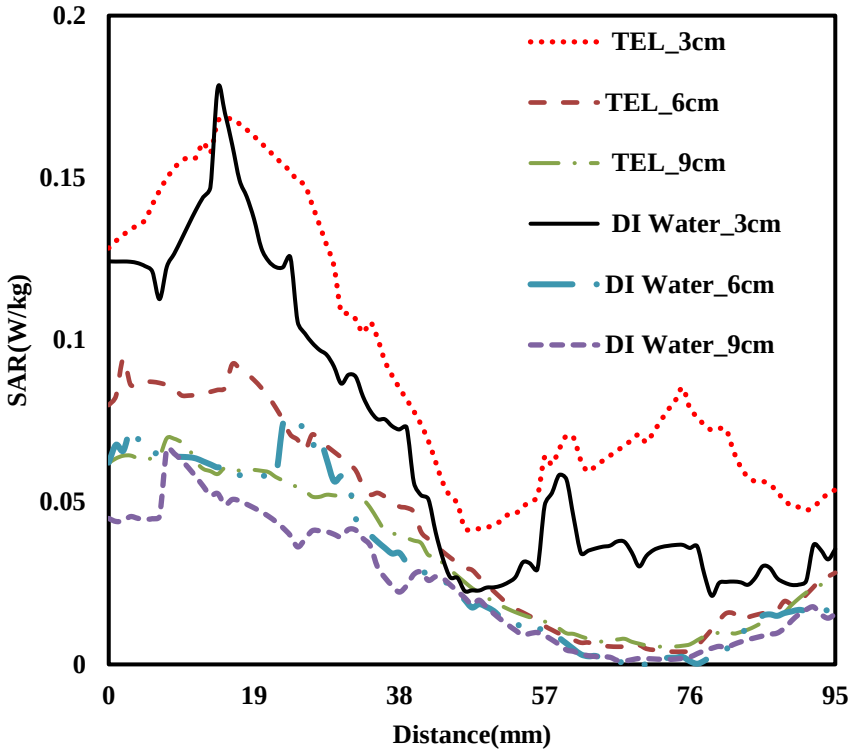


**Figure 4.4** Simulated SAR value

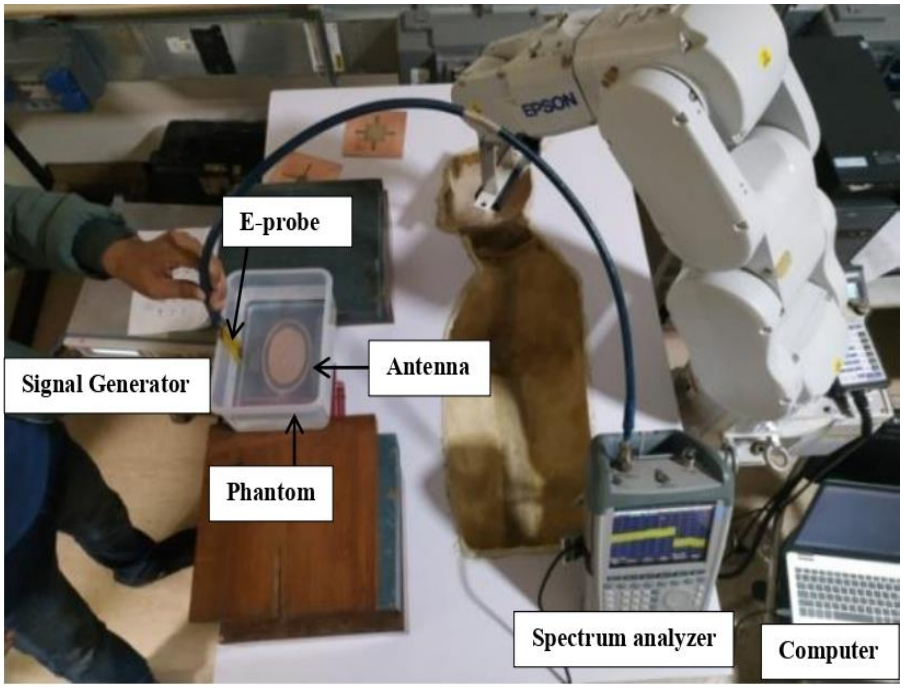


**Figure 4.5** Measurement setup for E-field strength

**Table 4.2** SAR calculation when the E- fields were measured along the x-axis

| Phantom Details | Distance b/w antenna and Phantom (d) in cm | Distance inside the Phantom ($x_1$) in cm | Measured E-Field strength at ($x_1$) V/m | SAR W/kg |
|---|---|---|---|---|
| DI Water | 3 | 5.0 | 12.6 | 0.10338 |
| | | 6.5 | 14.5 | 0.13692 |
| | | 8.0 | 13.3 | 0.11519 |
| | | 9.5 | 13.2 | 0.11347 |
| TEL | 3 | 5.0 | 78.1 | 5.08585 |
| | | 6.5 | 78.5 | 5.13808 |
| | | 8.0 | 59.2 | 2.92216 |
| | | 9.5 | 33.0 | 0.90801 |

### 4.4.3. Radiation Pattern

The elliptical-shaped ground-slotted antenna exhibits a distinctive radiation pattern characterized by dipole-like behavior, as depicted in Figure 4.6. This phenomenon is attributed to the presence of two nulls at 0 degrees and 180 degrees, indicative of the antenna's directional characteristics.

The incorporation of a slot in the ground plane introduces a novel mechanism for radiation leakage. This phenomenon is evident in the radiation pattern of the H-plane, where radiation is observed behind the ground plane. The presence of the slot facilitates the leakage of electromagnetic waves from the antenna structure, resulting in radiation beyond the conventional boundaries of the antenna aperture. The maximum realized gain of the antenna is determined to be -1 dB, indicating a slight reduction in power radiation compared to an ideal isotropic radiator. This reduction in gain may be attributed to factors such as impedance mismatches, losses in the antenna structure, and radiation inefficiencies.

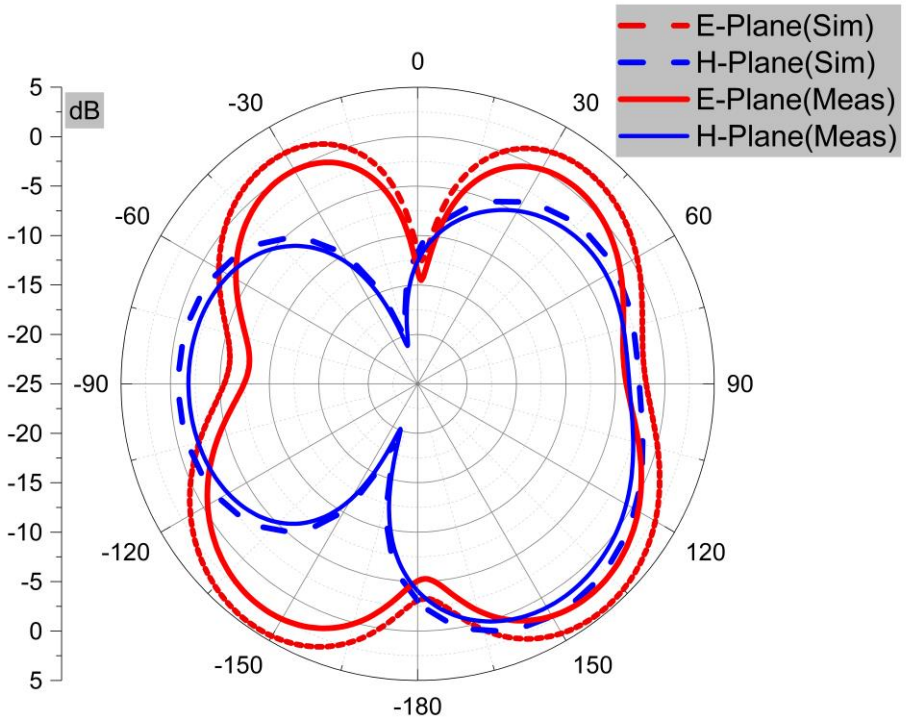


**Figure 4.6** Radiation pattern of the proposed elliptical antenna structure

**Table 4.3** Qualitative comparison of reported antennas to the proposed antenna

| Ref. | Frequency | $S_{11}$(dB) | SAR(W/kg) | Size(mm) | Application |
|---|---|---|---|---|---|
| [19] | 434 MHz | -13.8 | 1.32 | 130×130 ×2.97 | MICS |
| [56] | 434 MHz<br>915 MHz | -16<br>-17 | 1.32<br>1.44 | 124×124 ×1.6 | MICS<br>ISM |
| [113] | 915 MHz<br>2.45 GHz | -32<br>-27 | 11.17<br>27.93 | 120×120×2.007 | ISM |
| [123] | 2.45 GHz | -11 | Not reported | 29×29×0.5 | ISM |
| [124] | 400 MHz<br>2.4 GHz | -22<br>-26 | 241.5<br>149.5 | 3.14×100×2.54 | MICS<br>ISM |
| This work | 2.48 GHz | -15.1 | 5.138 | 128×128 ×1.58 | ISM |

From Table 4.3 it can be concluded that the proposed antenna operates at a higher ISM band i.e. at 2.48 GHz with a reflection coefficient of -15.1 dB and shows a better SAR value of 5.138 W/kg in the case of TEL phantom when the E-field strength is measured along the x-axis at a 6.5 cm depth of penetration than the antenna structure reported in [19, 56, 113, 123, 124].

## 4.5. Conclusion

In this work, a low-profile elliptical patch antenna was designed at 2.48 GHz for hyperthermia application. The antenna performance is compared at different distances from the phantom model using FEM modelling. SAR and reflection coefficient have been evaluated at 3 cm, 6 cm, and 9 cm to the antenna from the phantom. The simulated and measured values of the reflection coefficient are -15.1 dB and -14.9 dB respectively. The value of SAR lies in the permissible limit of the exposed body as stated by IEEE standards.

In the forthcoming Chapter 5, there is a pivotal aim to minimize the dimensions of ISM band antennas and improved SAR.